International Journal of Civil Engineering

Geotechnique

Use of line segments slip surface for optimized design of piles in stabilization of the earth slopes

M. Hajiazizi[1],*, A. R. Mazaheri[2]

Received: March 2014, Revised: June 2014, Accepted: November 2014

Abstract

Stabilization of earth slopes with various proposed methods is one of the important concerns of geotechnical engineering. In this practice, despite numerous developments, design conservativeness and high costs of stabilization are the issues yet to be addressed. This paper not only deals with pile location optimization but also studies the effects of the pile length by using line segments slip surface (non-circular). Taking into account the line segments slip surface in stabilization of earth slopes is a new topic which has been addressed in this paper. The line segments slip surface is actual slip surface and for determining the pile location it can lead to the actual length of the pile.

The line segments critical slip surface is obtained by using the Alternating Variable Local Gradient (AVLG) optimization method. AVLG is an approach in optimization process and it is based on the Univariate method. The line segments form the initial and critical slip surface. Pile improper installation and inadequate length not only fails to increase the factor of safety, but also reduces it. The analyses are performed using the limit equilibrium (LE) method. Results of these analyses are acceptable and are properly consistent with the results obtained by other researchers.

Keywords: *Stabilization of earth slopes, Line segments slip surface, Pile length, Pile location optimization.*

1. Introduction

What should be considered at the beginning of any stabilization process besides slope safety is the minimization of expenses. Therefore, excavation on slope upstream and/or filling slope downstream and/or moderating slope angle are the primary and effective stabilization methods. If these methods cannot provide the desirable factor of safety it would be necessary to put effort in other methods such as increasing soil strength parameters, draining surface water and sub-surface (ground) water at embankments, and installing retaining walls and piles. Implementation of these solutions is usually costly and sometimes in order to achieve a desirable factor of safety it is necessary to combine one or several methods. Anyway, the aforementioned solutions are aimed at mitigating the driving force behind ruptures and/or increasing resistive forces.

Slopes stabilization methods can be studied as empirical, analytical, and numerical methods. This classification has been so far used by researchers and has undergone numerous studies [1-4].

** Corresponding author: mhazizi@razi.ac.ir*

1 Department of Civil Engineering, Razi University, Taghe Bostan, Kermanshah, Iran

2 Department of Civil Engineering, Ph.D Student, Razi University, Taghe Bostan, Kermanshah, Iran

One of the methods used for improving resistive forces is the installation of piles in earth slopes [5-15]. However the cement grouting [16] and the stone column [17] are good methods for stabilization.

Installing piles for stabilizing susceptible earth slope is an effective way of preventing the imbalance of force and instability.

Stabilizing effect by using pile is provided by the passive resistance of the pile below the slip surface and load transfer from the sliding mass to the underlying stationary soil or rock formation through the piles due to soil arching mechanism [18-20].

Poulos [21] recommends the installation of stabilizing piles be located in the center of the failure surface to avoid any slope failure behind or in front of the pile. A constant soil Young's modulus that varies linearly with depth has been used along with an ultimate lateral pressure. For the practical use, Poulos [21] promoted the flow mode that creates the least damage effect of soil movement on the pile where the soil movement is larger than the pile deflection.

Won et al. [22] presented a numerical comparison of predictions by limit equilibrium analysis and 3D numerical analysis for a slope–pile system. The length of pile has been considered to be up to the end of embankment without any limitation.

Lee et al. [23] use the Bishop's method assumptions and suggest that the most effective locations for installing piles in homogenous soils are around the slope crown and

[DOI: 10.22068/IJCE.13.1.14]

toe. However, in the case of two-layer soils with lower layers denser than the upper layers the best location for a row piles would be around the middle of the slope or its crown. Ito and Matsui [5] as well as Hassiotis et al. [8] believe that the proximity of slope crown is the best location for pile installation.

Ausilio et al. [13] argue that the most appropriate location for pile installation is in the vicinity of slope toe, where the minimum pile-induced force acts. The following issues are taken into account in the slope stabilization process: the effect of the distance between piles on factor of safety, effect of the poor soil layer on factor of safety, location of the critical failure surface, effect of alteration of the elasticity modulus on factor of safety, and the most effective and suitable place for pile installation. Ausilio et al. [13] propose a pile length two times the height of the pile above the slip surface. Usually, circular slip surface is used for methods based on LE method. Also Sun et al. [24] proposed a new design method for micro-piles for earth slope stabilization that includes details about choosing a location for the micro-piles within the existing slope, selecting micro-pile cross section, estimating the length of the micro-pile, evaluating the shear capacity of the micro-piles group, calculating the spacing required to provide force to stabilize the slope and the design of the concrete cap beam.

This paper studies the location optimization and length of pile with respect to line segments (non-circular) slip surface by using the LE method and based on AVLG method. The AVLG method has been described in reference [25] completely.

2. DOSS Software for Determining Non-Circular Critical Slip Surface Using LE Method

DOSS software [26] is written by authors for obtaining the non-circular critical slip surface. For obtaining the non-circular critical slip surface that is more consistent with the actual slip surface in the nature is used the Alternating Variable Local Gradient (AVLG) optimization method. The AVLG method is a new approach to the optimization of line-segments slip surface for the two- and three-dimensional state. Hajiazizi and Tavana [25] extended the AVLG method for the three-dimensional state. However, the present manuscript implemented this method for the two-dimensional state by using DOSS program.

2.1. Alternating variable local gradient method [25]

The AVLG method is based on the theory underlying the Univariate method [27]. In this method, one variable is moved in order to be optimized while the other variables remain fixed. Then, another variable is selected for optimization while the other variables again remain fixed. This process continues until all the variables are optimized by the end of the first cycle. Then, the optimization process of the second cycle is initiated. This process is also iterated until the movement of variables in the new cycle has no effect on the optimization of the objective function (safety factor).

The Univariable optimization method is a non-linear optimization method that is capable of optimizing non-linear functions based on Cauchy's theorem [28] and one by one movement of variables in the opposite direction of gradient. The factor of safety function is a non-linear function with nodes on the line-segment slip surface as its variables. According to Cauchy's theorem [28], as the slip surface nodes move in the opposite direction of the gradient of the same nodes, the value of the target function (i.e. factor of safety) reduces. Line segment slip surface is more capable of adjusting to the natural slip surface. Hence, using this slip surface the actual required length of pile is obtained.

In sum, the AVLG method for finding the most critical line segments (non-circular) slip surface can be expressed as follows:

Set i=1 (for starting of optimization process)

Finding the circular critical slip surface using the Grid Search method, or any other method, and taking it as the initial slip surface.

In the stability analysis of earth slopes, the safety factor is usually obtained by comparing a large number of slip surfaces and selecting the most critical slip surface. The DOSS software is capable of drawing many circular slip surfaces and selecting the surface with the minimum safety factor as the critical slip surface. Every circular slip surface has three control parameters which include the beginning of the slip surface, the end of the slip surface and the slip radius centers. The aforementioned control parameters are the inputs for drawing slip surface circles (Fig. 1). Next, for every slip surface, the factor of safety is obtained using the limit equilibrium method. The slip surface with the minimum factor of safety is called the critical slip surface. Unlike some softwares that define the radius of slip circles as one of the main variables, in the DOSS software other variables (e.g. coordinates of the start and end points of the slip surface) are defined to accelerate convergence and reduce the duration. Therefore, primary and additional calculations for circles crossing the slope between the beginning and ending points are avoided.

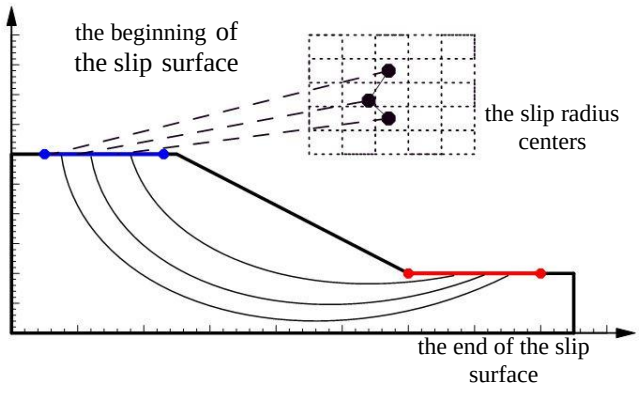

Fig. 1 The beginning of the slip surface and the end of the slip surface for finding critical slip surface

Selecting proper nodes on the circular critical slip surface and connecting them to each other (the number of

[DOI: 10.22068/IJCE.13.1.14]

the selected nodes plays a significant role in the optimization process. It is recommended to select more nodes on the weak layers in non-homogeneous soils). $\boldsymbol{Z}_i$ denotes the coordinates of the initial selected nodes.

$$\boldsymbol{Z}_i = (x_1, y_1, x_2, y_2, \dots, x_n, y_n) \quad (1)$$

Finding the best location for the first node on the slope boundary.

The new coordinates of slip surface are as follows:

$$\boldsymbol{Z}_i^* = (x_1^*, y_1^*, x_2, y_2, \dots, x_n, y_n) \quad (2)$$

In order to calculate the factor of safety the limit equilibrium method is employed. The factor of safety is calculated using the Janbu's method as follows,

$$\mathrm{FS} = f_0 \frac{1}{\sum_{i=1}^{n} \mathrm{W}_i \tan\alpha_i} \sum_{i=1}^{n} \{\mathrm{C}' \Delta x_i + (\mathrm{W}_i - \mathrm{u}_i \Delta x_i) \tan\phi_i'\} \left\{ \frac{\sec^2 \alpha_i}{1 + \tan\alpha_i \frac{\tan\phi_i'}{\mathrm{FS}}} \right\} \quad (3)$$

where,

n = No. of slices

$\tan\alpha_i = (y_{i+1} - y_i)/(x_{i+1} - x_i)$

W_i = weight of the i-th slice

C' = cohesion

ϕ' = friction angle of soil

α_i = angle of inclination of the slip surface for i-th slice

$y_{i+1}, y_i, x_{i+1}, x_i, f_i, f_{i+1}$ illustrated in Fig. 2.

f_0= correction factor

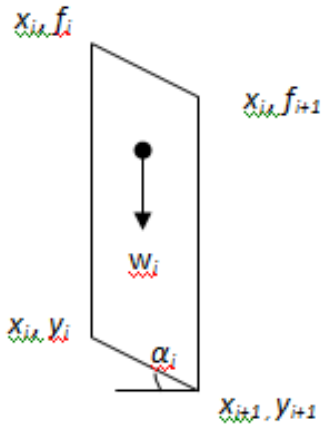

Fig. 2 One slice and its coordinates

Finding the best location for the next node of the slip surface while also keeping the other nodes fixed results in a lower factor of safety. The best location for each internal node is obtained by its moving in the negative direction of the local gradient vector. The relation for the negative direction of the local gradient vector is as follows:

$$\boldsymbol{S}_k = -\boldsymbol{G}_k = -\left\{\frac{\partial Fs}{\partial x_k}, \frac{\partial Fs}{\partial y_k}\right\}^T \quad (4)$$

Fig. 3 shows node 2 and the route in the negative direction of its local gradient vector.

For example, node 2 moves from its initial coordinates, (x_2, y_2), to its new coordinates, (x^*_2, y^*_2), where it yields a lower safety factor. Thus, the new coordinates of the slip surface are as follows:

$$\boldsymbol{Z}_i^* = (x_1^*, y_1^*, x_2^*, y_2^*, x_3, y_3, \dots, x_n, y_n) \quad (5)$$

Finding the best location for the subsequent internal node while other nodes remain fixed. This process is iterated for the rest of the internal nodes. The new coordinates of the slip surface are as follows:

$$\boldsymbol{Z}_i^* = (x_1^*, y_1^*, x_2^*, y_2^*, \dots, x_k^*, y_k^*, \dots, x_n, y_n) \quad (6)$$

Find the best location for the last node on the slope boundary. In this step the first optimization cycle is terminated. The new coordinates of the slip surface are as follows:

$$\boldsymbol{Z}_{i+1}^* = (x_1^*, y_1^*, x_2^*, y_2^*, \dots, x_{n-1}^*, y_{n-1}^*, x_n^*, y_n^*) \quad (7)$$

Set i=i+1

Steps 4 to 7 are repeated for several cycles until the difference between the safety factors of the last two cycles is less than $\varepsilon=1\times10^{-5}$. Or

$$|FS(\mathbf{Z}_{i+1}^*) - FS(\mathbf{Z}_i^*)| < \varepsilon \quad (8)$$

FS ($\mathbf{Z}^*_{i+1}$) = the factor of safety for the last optimization cycle,

FS ($\mathbf{Z}^*_i$) = the factor of safety for the penultimate optimization cycle.

The slip surface associated with the last factor of safety is taken as the most critical slip surface.

3. Example 1

The inclined surface studied in this example is depicted in Fig. 4. The embankment height is equal to 13.7 m and its gradient is equal to 30 degrees. The unit weight is 19.63 kN/m^3, angle of internal friction is 10 degrees, cohesion is equal to 23.94 kN/m^2, modulus of elasticity is 12000 kN/m^2, and Poisson's ratio is equal to 0.3.

[DOI: 10.22068/IJCE.13.1.14]

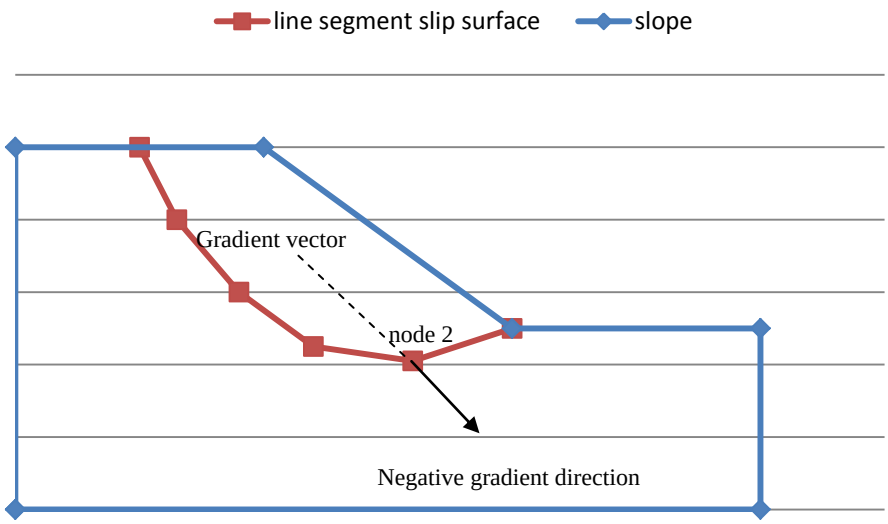

Fig. 3 Only one node is moved along the local gradient negative direction and other nodes are fixed

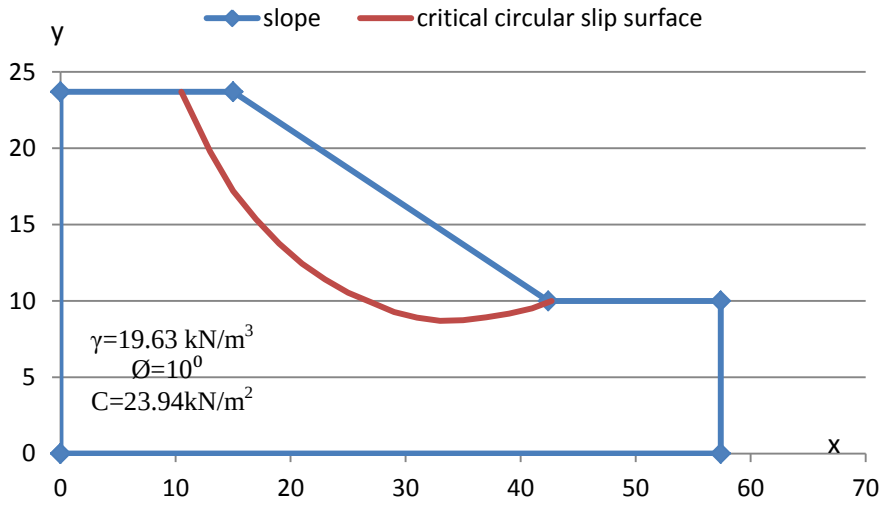

Fig. 4 Slope geometry and critical circular slip surface in example 1

3.1. Determining the most critical slip surface without a row of piles

This problem has been solved by [8, 13,15] as well. In this paper the most critical slip surface and its associated factor of safety are determined using the LE method. Results of this research properly comply with the results of other researches shown in Tab. 1 before installing the piles. The output of the Fellenius' method [29] is also added to Table 1.

Table 1 Critical safety factor for different methods in example 1 before pile

In This paper	Previous Analysis			
LEM	Xinpo Li et al [15]	Ausilio et al [13]	Hassiotis et al. [8]	Fellenius [29]
1.11	**1.11**	**1.11**	**1.08**	**1.05**

Fig. 4 shows the circular critical slip surface as well. The calculated safety factor of the circular slip surface is 1.11. This circular slip surface is the most critical slip surface in the earth slope showed in Fig. 4. This slip surface is taken as the initial slip surface, which is used for optimization and on which an appropriate number of nodes should be selected. In this example, 12 nodes are selected on the circular critical slip surface (Fig. 5). Nodes are connected to each other by means of lines, and thus form the initial non-circular slip surface (Fig. 5). The optimization process is repeated for all nodes in each cycle until the factor of safety of that cycle is decreased. Each node moves in the negative direction of its local gradient vector until it reaches the best location, which gives the lower factor of safety. In fact, with reduction of the safety factor in each cycle the objective function is optimized. As seen in Fig. 6, in the first optimization cycle the value of the safety factor decreases until it reaches value 1.0878. The optimization process continues until the minimum factor of safety is obtained in the fourth cycle (Fig. 6). Fig. 6 shows the four cycles along the horizontal axis and the constancy of the safety factor during the last two cycles. The obtained minimum factor of safety is equal to 1.0545.

[DOI: 10.22068/IJCE.13.1.14]

The difference between the safety factor of the last two cycles (cycles 3 and 4) is less than $1*10^{-5}$. Therefore, the optimization process is terminated. Fig. 7 shows the initial and critical non-circular slip surface (FS=1.0545), which is obtained after the optimization of the initial slip surface.

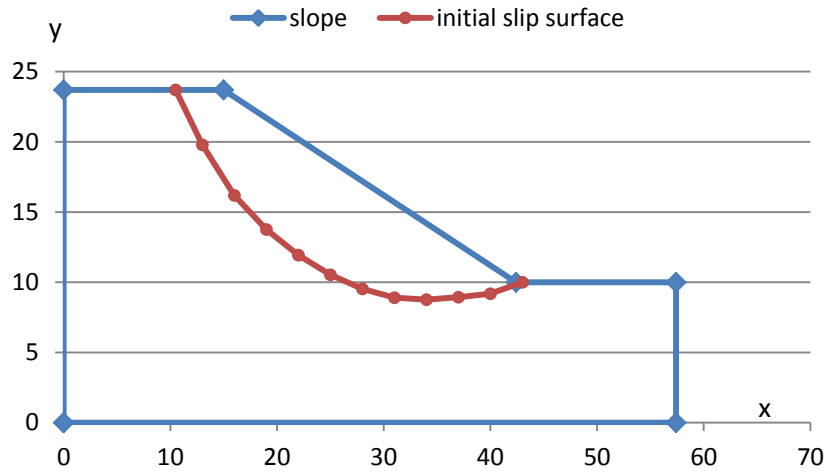

Fig. 5 Initial slip surface on the circular slip surface in example 1

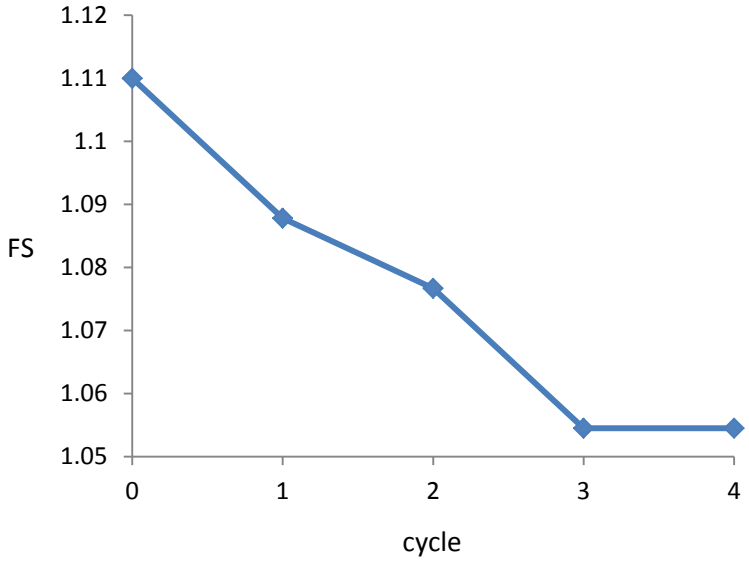

Fig. 6 The value of safety factor at the end of each cycle

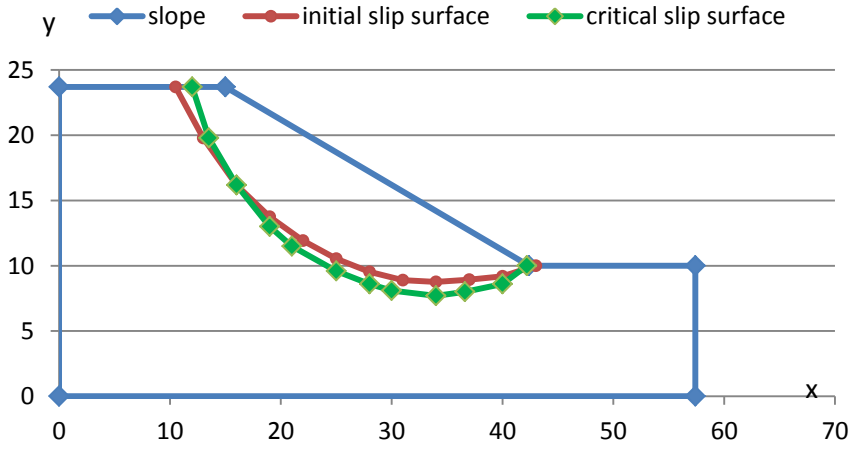

Fig. 7 Initial and critical slip surface after four cycle optimization

[DOI: 10.22068/IJCE.13.1.14]

3.2. Analysis of the effects of pile location and length

It is possible to increase the factor of safety by installing a row of piles in an appropriate place. Piles with varying lengths of $L=H$, $L=1.5H$, and $L=2H$ installed in different locations (x/r) between the slope toe and crown are modeled here (Fig. 8). The length values (L) for a pile with a diameter of 1 m installed in different locations (x/r) are presented in Table 2. In order to apply the pile bearing capacity to shear strength, reference [30] was used. Following the installation of the pile, the value of factor of safety increases. This increase is the result of the growth of a resisting force produced by the pile against movement. The relation for factor of safety following the installation of the pile is as follows,

$$SF_T = \frac{F_C + F_P}{F_W}$$

where

F_C=the resisting force of soil mass

F_W=the driving force of soil mass

F_P=the total resistance provided by piles

F_P is the force of the triangular load that a cantilever beam (pile) can bear to demonstrate an allowable degree of deformation. In fact, beam stiffness determines the geometrical dimensions of the pile so that the pile shows bearing capacity of F_P and allowable displacement.

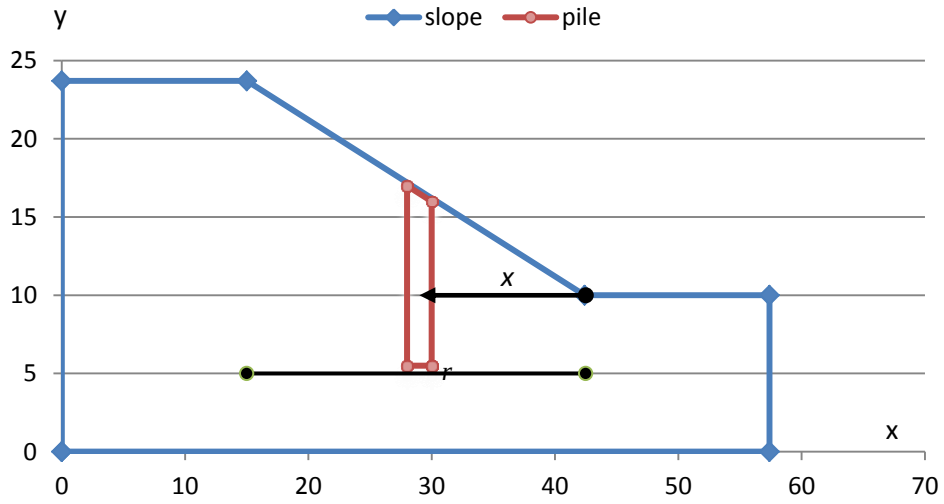

Fig. 8 Location of pile between the toe and crown

Table 2 The pile length (L) in different locations (x/r)

x/r	*L=H*	*L=1.5H*	*L=2H*
0.1	2.4	3.6	4.8
0.2	3.7	5.5	7.4
0.3	5.3	7.9	10.6
0.4	6.4	9.6	12.8
0.5	7.5	11.3	15.1
0.6	8	12	16
0.7	8.1	12.1	16.2
0.8	8.1	12.1	16.2

Fig. 9 shows the variations of safety factor obtained for different pile locations using the LE method (L=2H). As seen in this figure, in order to achieve the largest factor of safety in a homogenous soil using the LE method the pile should be installed near the slope middle(x/r=0.4). After installing the pile on a homogeneous soil, the critical slip surface moves below the pile and the factor of safety reaches 1.36 (Fig. 10).

When the pile tip is located into dense layer (such as bedrock) the safety factor (FS=1.697) increases significantly, as shown in Fig. 11 (for L=1.5H). After embedding the pile tip into a dense layer, the critical slip surface cuts the pile and the factor of safety reaches 1.697 (Fig. 12).

[DOI: 10.22068/IJCE.13.1.14]

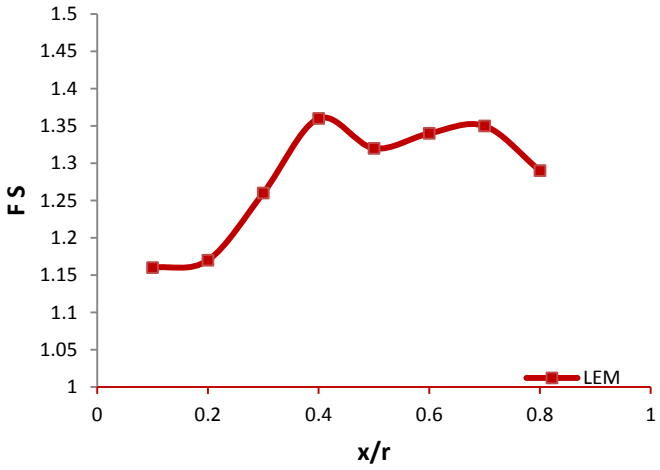

Fig. 9 Variations of safety factor obtained for different locations and L=2H

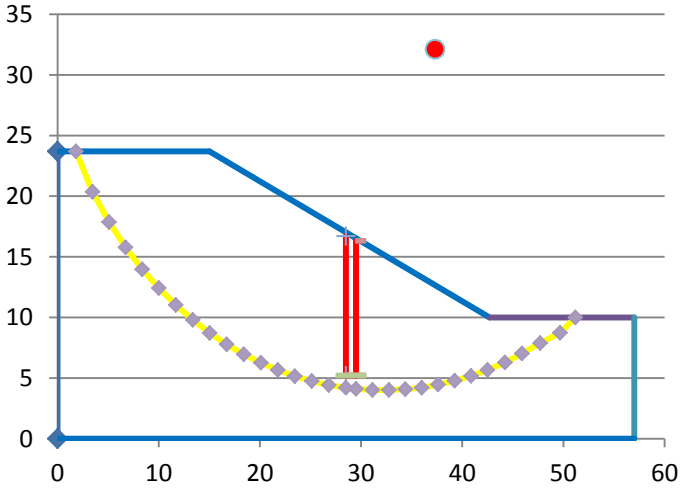

Fig. 10 Critical slip surface and optimal location of pile in homogeneous soil (example 1)

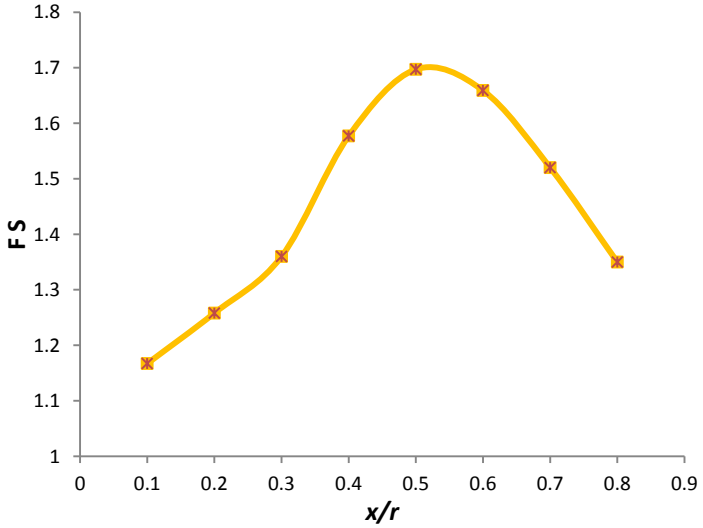

Fig. 11 The pile tip is located in the dense layer and safety factor increases for L=1.5H

[DOI: 10.22068/IJCE.13.1.14]

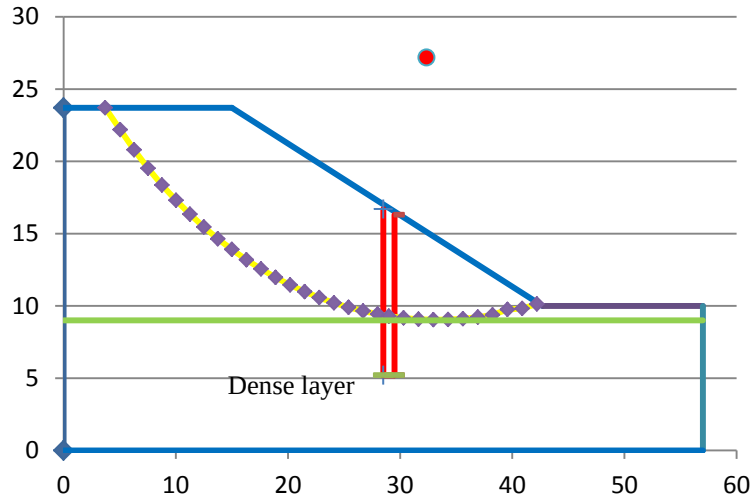

Fig. 12 Critical slip surface and optimal location of pile when the pile tip is located into a dense layer

Results of reference [15] with a length of 2H and this paper with a length of 1.5*H* performed using the LE method (when the pile tip is located in a dense layer) are also presented in Fig. 13 and it yield the largest factor of safety at *x*/*r*=0.5. According to Fig. 13, when the pile tip is located into dense layer the safety factor (FS=1.697) increases, however the pile length has been decreased. It is notable that in order to install a pile on a slope side, the access road is constructed on the downstream (and not the upstream) of the pile installation site. That is to say, after determining the pile installation location, it is necessary to create an access road on the downstream of the pile location. The reason is that on the downstream the weight of machinery has the lowest effect on slope stimulation.

3.3. Determining the most effective location for pile installation

The most effective location for pile installation is the place that not only gives the required factor of safety but also uses the minimum pile length. As seen in Fig. 14 a horizontal plane can give the required factor of safety (for example FS=1.1). The point the plane collides with the curve gives the coordinates of different pile lengths and locations. The place with the shortest pile length is the most effective for pile installation.

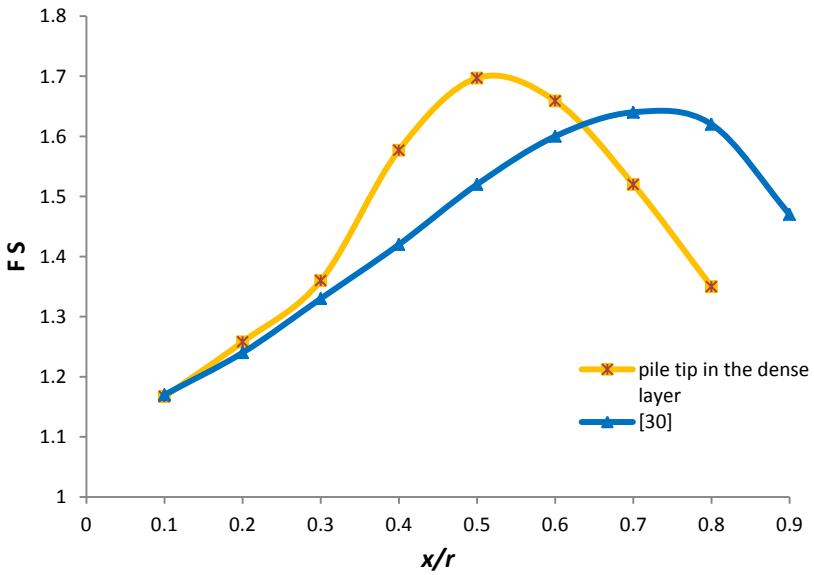

Fig. 13 Comparison of reference [30] with a length of 2*H* and this paper when the pile tip is located in a dense layer with a length of 1.5*H*

[DOI: 10.22068/IJCE.13.1.14]

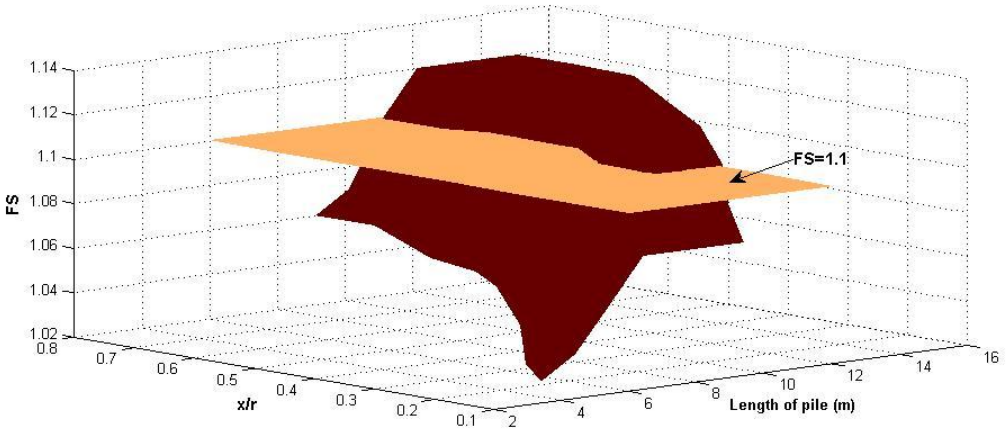

Fig. 14 Three dimensional diagram of pile length (*L*), pile location(*x/r*) and factor of safety (*FS*) in example 1

4. Example 2

The three-layer earth slope studied in this example is depicted in Fig. 15. The strength parameters of the third layer are larger than those of the other two layers. The slope height is 10 m and its angle is 34 degrees. The physical characteristics of the layers are presented in Table 3.

Table 3 The strength parameters of earth slope in example 2

Layer No.	Cohesion (kPa)	Friction Angle (degree)	Unit Weight (kN/m^3)	Poisson's Ratio	Elasticity Modulus (kN/m2)
Layer 1	29.43	12	18.8	0.3	12000
Layer 2	9.81	5	18.8	0.3	12000
Layer 3	294.3	40	18.8	0.3	12000

4.1. Determining the most critical slip surface without a row piles

Fig. 16 shows the circular critical slip surface. The calculated safety factor of the circular slip surface is 0.88. This slip surface is taken as the initial slip surface, which is used for optimization and on which an appropriate number of nodes should be selected. In this example, 8 nodes are selected on the circular critical slip surface (Fig. 17). Nodes are connected to each other by means of lines, and thus form the initial non-circular slip surface (Fig. 17). The optimization process is repeated for all nodes in each cycle until the factor of safety of that cycle is decreased. Each node moves in the negative direction of its local gradient vector until it reaches the best location, which gives the lower factor of safety. In fact, with reduction of the safety factor in each cycle the objective function is optimized. The optimization process continues until the minimum factor of safety is obtained in the third cycle. The obtained minimum factor of safety is equal to 0.844.

The difference between the safety factor of the last two cycles (cycles 2 and 3) is less than $1*10^{-5}$. Therefore, the optimization process is terminated. Fig. 18 shows the initial and critical non-circular slip surface, which is obtained after the optimization of the initial slip surface.

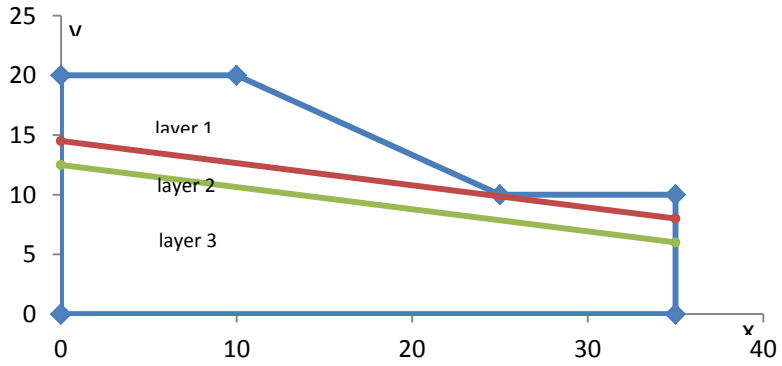

Fig. 15 Three-layer earth slope geometry in example 2

[DOI: 10.22068/IJCE.13.1.14]

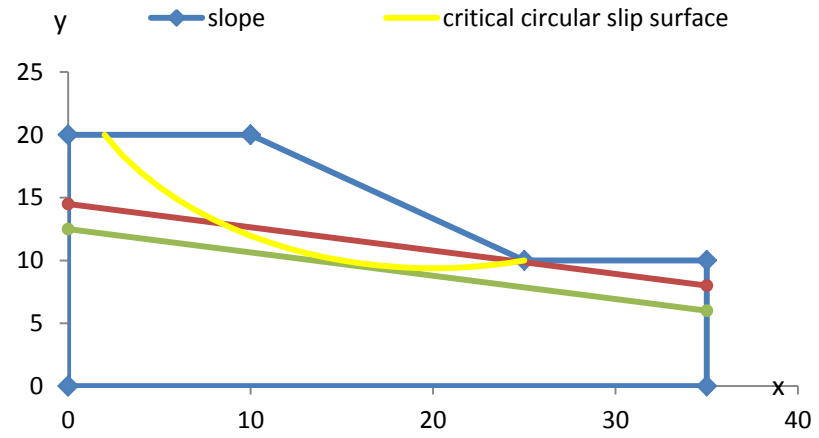

Fig. 16 The circular critical slip surface in example 2

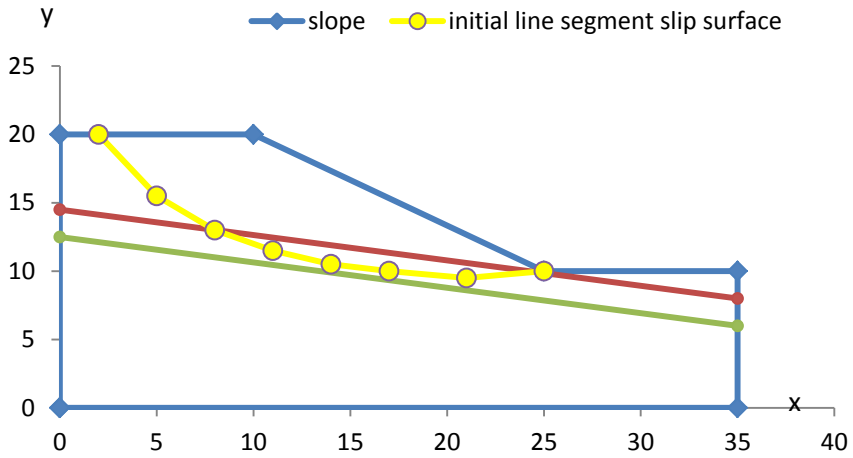

Fig. 17 Initial slip surface on the circular slip surface in example 2

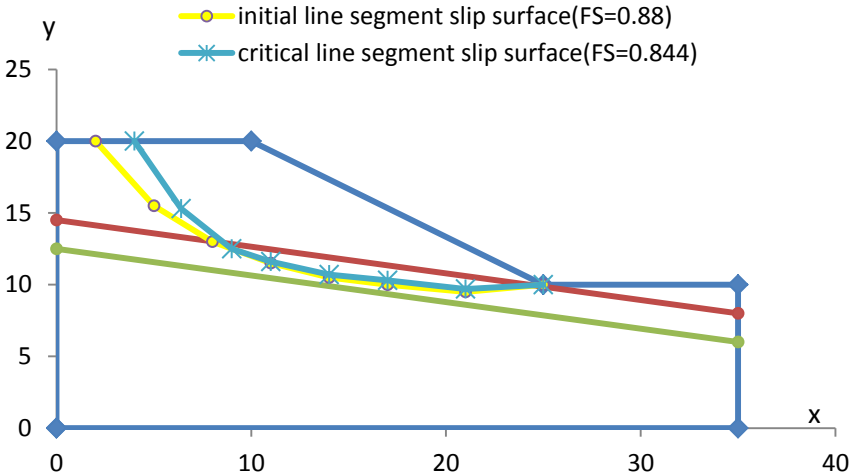

Fig. 18 Initial and critical slip surface after three cycle optimization

4.2. Analysis of the effects of pile location and length on stability analysis

It is possible to increase the factor of safety by installing a row of piles. Different locations of piles with varying lengths of $L=H$, $L=1.5H$, and $L=2H$ installed in different locations (x/r) between the slope toe and crown are modeled and analyzed (Fig. 19). The length values for a pile with a diameter of 1 m installed in different locations (x/r) are presented in Table 4.

[DOI: 10.22068/IJCE.13.1.14]

Table 4 The pile length (L) in different locations (x/r) in example 2

x/r	$L=H$ (m)	$L=1.5H$ (m)	$L=2H$(m)
0.1	2	3	4
0.2	3.25	4.87	6.5
0.3	4.3	6.45	8.6
0.4	5	7.5	10
0.5	5.8	8.7	11.6
0.6	6.2	9.3	12.4
0.7	6.5	9.75	13
0.8	7	10.5	14

Results of the slope stability analysis of a row of piles with diameters of 1 m and lengths of 2H performed using the LE method are also presented in Fig. 20. According to Fig. 20 the LE method yield the largest factor of safety (FS=1.67) at x/r=0.4.

Results of the slope stability analysis with lengths of 1.5H performed using the LE method is also presented in Fig. 21. Comparison of Figs. 20 and 21show no difference between factor of safety with lengths of 1.5H and 2H when pile tip is located into dense layer. The figure of the optimal location of pile and the critical slip surface shows in Fig. 22.

Results of the variations of reliability length (L_e) (Fig. 23) are depicted in Fig. 24. The maximum factor of safety (FS=1.63) is also achieved with $L=H+4D$ and with length values higher than $H+4D$ the factor of safety remains unchanged. The increase in the factor of safety is a result of the collision between pile tip and the dense layer.

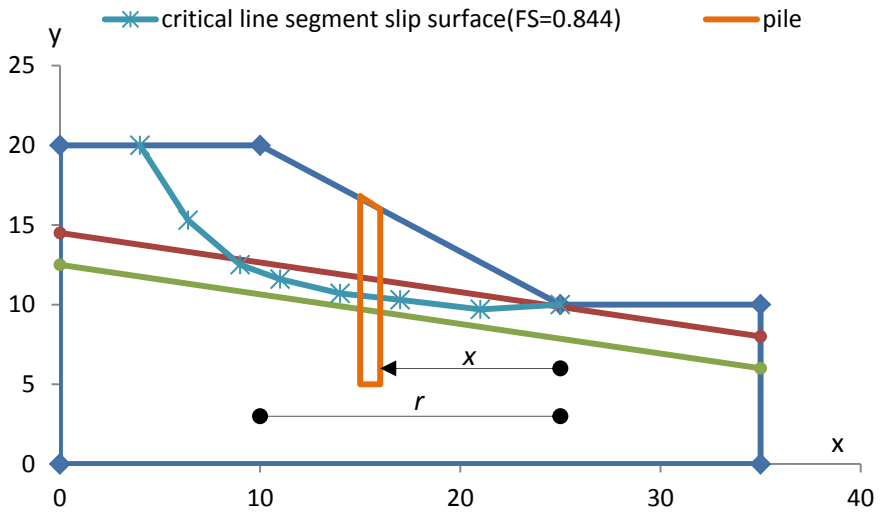

Fig. 19 Pile location (x/r) between the toe and crown

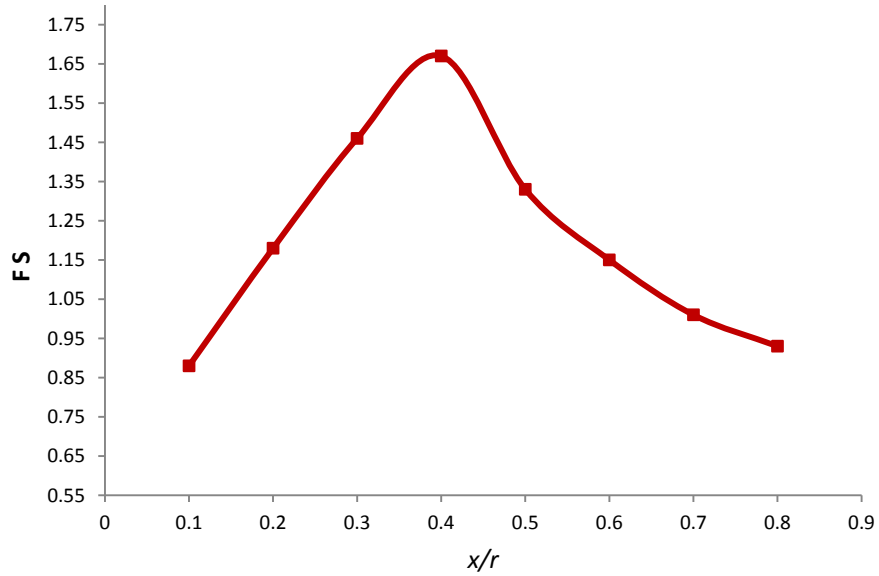

Fig. 20 Variations of safety factor obtained for different locations and $L=2H$

[DOI: 10.22068/IJCE.13.1.14]

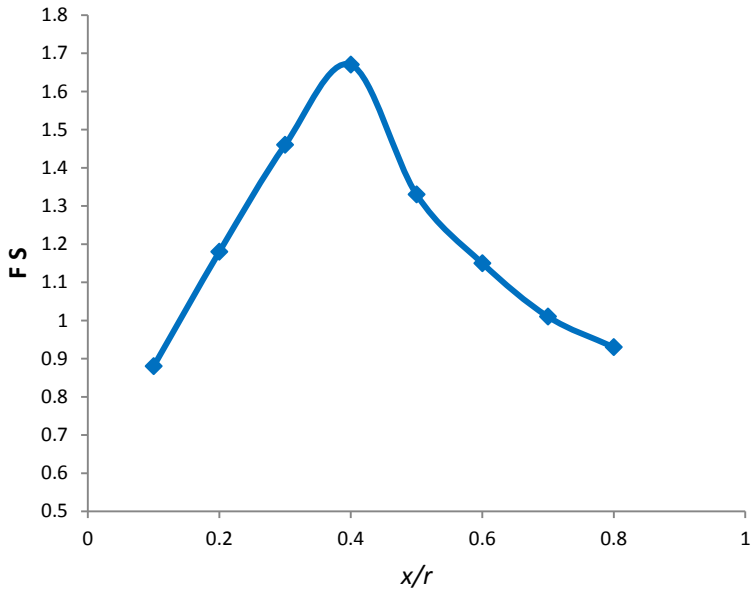

Fig. 21 Variations of safety factor obtained for different locations and L=1.5H

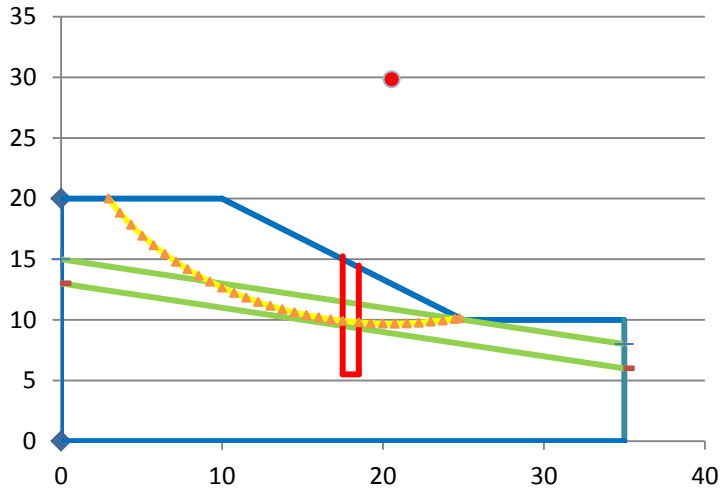

Fig. 22 Critical slip surface and optimal location of pile

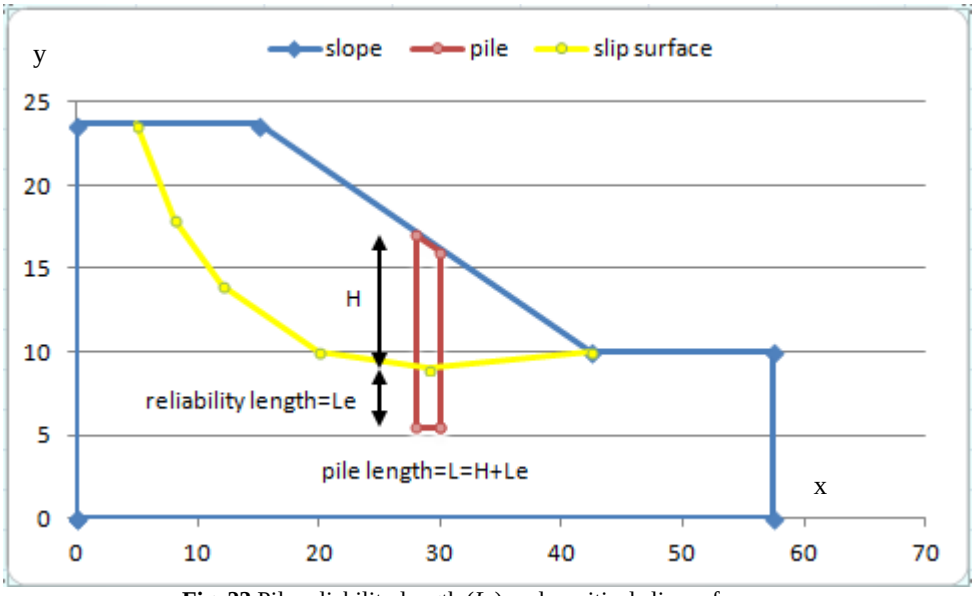

Fig. 23 Pile reliability length (L_e) under critical slip surface

[DOI: 10.22068/IJCE.13.1.14]

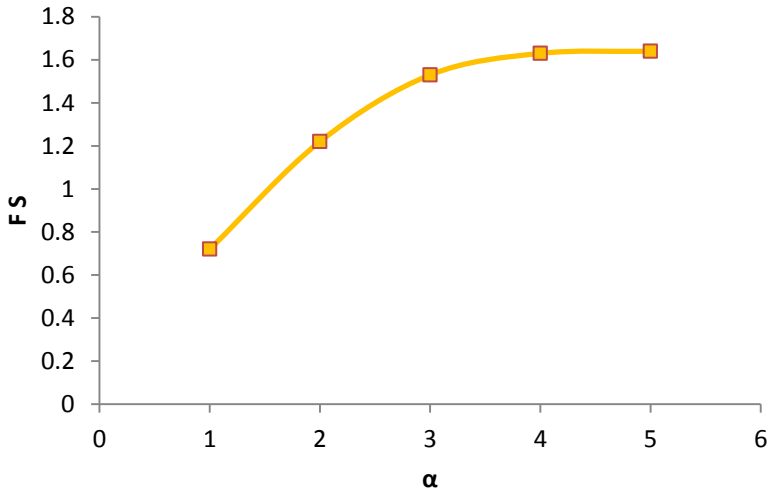

Fig. 24 Variations of pile reliability length ($L_e=\alpha D$) and factor of safety

4.3. Determining the most effective location for pile installation

Fig. 25 shows the three-dimensional diagram of pile length (L), pile location (x/r), and factor of safety (FS). In order to find the most effective location for pile installation the horizontal plane for the factor of safety of interest (for example FS=1.3) should be mapped. The most effective location is the one that requires the shortest pile length. In fact, not only the most effective location yields the required factor of safety but also provides for the shortest pile length and reduction in stabilization costs.

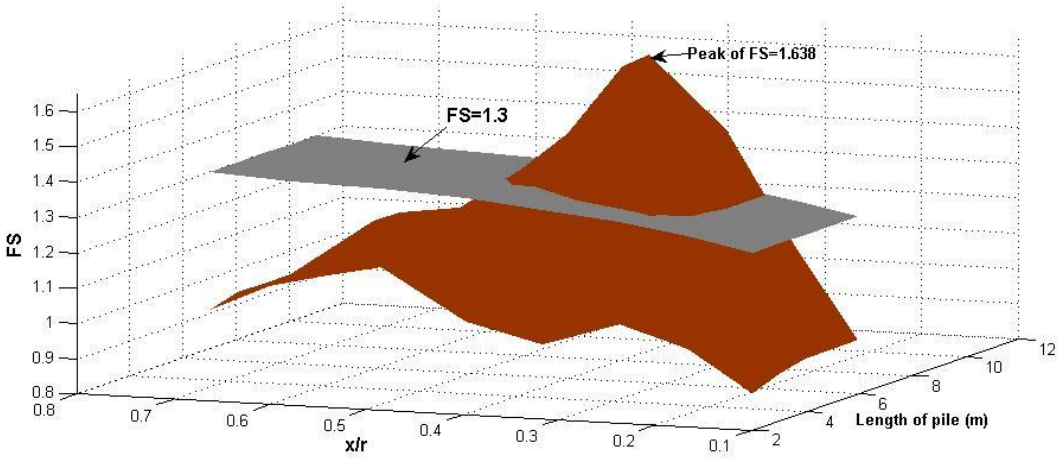

Fig. 25 Three-dimensional diagram of pile length (L), pile location (x/r), and factor of safety

5. Conclusion

In this paper the line segments slip surface is used for determining of minimum safety factor which has been addressed in this paper as a new topic. Line segment slip surface is more consistent with the natural slip surface. Therefore, the required length of pile used for reinforcement purposes is obtained with more precision. Locating pile tip in a dense layer is a method that helps to increase safety factor and reduce stabilization costs, significantly. Then it is necessary to find a dense layer in the bottom layers of slope if possible. In order to achieve the maximum factor of safety for a row of piles in homogenous slopes the piles should be installed in the vicinity of slope middle. Most numerical and experimental studies recommend slope center as the best place for pile installation. The present research also gave the same result using the line segment slip surface. Increasing pile length into soil in homogenous slopes can't increase factor of safety significantly. If the piles are installed in the inappropriate location and the inadequate length, the factor of safety is decreased instead of being increased.

Locating pile tip into dense layer in homogenous slopes can increase factor of safety by 30%. As a result, pile length and consequently stabilization costs are reduced. If the tip of a pile in a non-homogeneous slope is emplaced into a dense layer, the required reliability length

[DOI: 10.22068/IJCE.13.1.14]

will be achieved. However, if the pile tip is embedded into a soft layer, fixing the pile tip using soil improvement will have a considerable effect on increasing the factor of safety. Three-dimensional graphs of pile length-pile location-safety factor are capable of selecting the shortest pile length to obtain the desired safety factor and thus reduce reinforcement costs.

References

[1] Zeng S, Liang RY. Stability analysis of drilled shafts reinforced slope, Soils and Foundations, 2002, No. 2, Vol. 42, pp. 93-102.

[2] Liang RY, Yamin MM. Three-dimensional finite element study of arching behavior in slope/drilled shafts system, International Journal for Numerical and Analytical Methods in Geomechanics, 2009, No. 11, Vol. 34, pp. 1157-1168.

[3] Kim J, Salgado R, Lee J. Stability analysis of complex soil slopes using limit analysis, Journal of Geotechnical and Geoenvironmental Engineering, 2002, No. 7, Vol. 128, pp. 546-557.

[4] Oakland MW, Chameau JLA. Finite-element analysis of drilled piers used for slope stabilization, Laterally loaded deep foundations, ASTM, West Conshohoken, PA, 1984, pp. 182–193.

[5] Ito T, Matsui T. Methods to estimate lateral force acting on stabilizing piles, Soils and Foundations, 1975, No. 4, Vol. 15, pp. 43-60.

[6] Poulos HG. Design of reinforcing piles to increase slope stability, Canadian Geotechnical Journal, 1995, No. 5, Vol. 32, pp. 808-818.

[7] Jeong S, Kim B, Won J, Lee J. Uncoupled analysis of stabilizing piles in weathered slopes, Computers and Geotechnics, 2003, No. 8, Vol. 30, pp. 671-682.

[8] Hassiotis S, Chameau JL, Gunaratne M. Design method for stabilization of slopes with piles, Journal of Geotechnical and Geoenvironmental Engineering, 1997, No. 4, Vol. 123, pp. 314-323.

[9] Chow YK. Analysis of piles used for slope stabilization, International Journal for Numerical and Analytical Methods in Geomechanics, 1996, No. 9, Vol. 20, pp. 635-646.

[10] Cai F, Ugai K. Numerical analysis of the stability of a slope reinforced with piles, Soils and Foundations, 2000, No. 1, Vol. 40, pp. 73-84.

[11] Kourkoulis R, Gelagoti F, Anastasopoulos I, Gazetas G. Slope stabilizing piles and pile-groups: Parametric study and design insights, Journal of Geotechnical and Geoenvironmental Engineering, 2011, No. 7, Vol. 137, pp. 663-678.

[12] Kourkoulis1 R, Gelagoti F, Anastasopoulos I, Gazetas G. Hybrid method for analysis and design of slope stabilizing piles, Journal of Geotechnical and Geoenvironmental Engineering, 2012, No. 1, Vol. 138, pp. 1-14.

[13] Ausilio E, Conte E, Dente G. Stability analysis of slopes reinforced with piles, Computers and Geotechnics, 2001, Vol. 28, pp. 591-611.

[14] Ito T, Matsui T, Hong WP. Extended design method for multi-row stabilizing piles against landslide, Soils and Foundations, 1982, No. 1, Vol. 22, pp. 1-13.

[15] Xinpo Li, Xiangjun Pei, Marte Gutierrez, Siming He. Optimal location of piles in slope stabilization by limit analysis, Acta Geotechnica, 2012, Vol. 7, pp. 253-259.

[16] Heidarzadeh M, Mirghasemi AA, Sadr Lahijani SM. Application of cement grouting for stabilization of coarse materials, International Journla of Civil Engineering, 2013, No. 1, Vol. 11, pp. 71-77.

[17] Nazari Afshar J, Ghazavi M. a simple analytical method for calculation of bearing capacity of stone-column, International Journla of Civil Engineering, 2014, No. 1, Vol. 12, pp. 15-25.

[18] Chen LT, Poulos HG, Hull TS. Model tests on pile groups subjected to lateral soil movement, Soils and Foundations, 1997, No. 1, Vol. 37, pp. 1-12.

[19] Chen CY, Martin GR. Soil-structure interaction for landslide stabilizing piles, Computers and Geotechnics, 2002, No. 5, Vol. 29, pp. 363-386.

[20] Liang R, Zeng S. Numerical study of soil arching mechanism in drilled shafts for slope stabilization, Soils and Foundations, 2002, No. 2, Vol. 42, pp. 83-92.

[21] Poulos HG. Design of reinforcing piles to increase slope stability, Canadian Geotechnical Journal, 1995, No. 5, Vol. 32, pp. 808-818.

[22] Won J, You K, Jeong S, Kim S. Coupled effects in stability analysis of pile-slope systems, Computers and Geotechnics, 2005, Vol. 32, pp. 304-315

[23] Lee CY, Hull TS, Poulos HG. Simplified pile-slope stability analysis, Computers and Geotechnics, 1995, Vol. 17, pp. 1-16.

[24] Sun SW, Zhu BZ, Wang JC. Design method for stabilization of earth slopes with micropiles, Soils and Foundations, 2013, Issue 4, Vol. 53, pp. 487‑497.

[25] Hajiazizi M, Tavana H. Determining three-dimensional non-spherical critical slip surface in earth slopes using an optimization method, Engineering Geology, 2013, Vol. 153, pp. 114-124.

[26] DOSS program, Software of Determination of Optimal Slip Surface, Razi University, Iran, 2010.

[27] Rao SS. Optimization Theory and Applications, Wiley Eastern Limited, India, 1991, pp. 70-100.

[28] Cauchy AL. Method general pour la resolution des system d' equations simultanees, CR Acad. Science, Paris, 1847, Vol. 25, pp. 536-538.

[29] Harr ME. Foundations of Theoretical Soil Mechanics, McGrw Hill, 1996.

[30] Ashour M, Ardalan H. Analysis of pile stabilized slopes based on soil–pile interaction, Computers and Geotechnics, 2012, Vol. 39, pp. 85-97.

[DOI: 10.22068/IJCE.13.1.14]